Transition mechanisms and spectral shapes of the $^5D_0$-$^7F_0$ line of Eu^{3+} and Sm^{2+} in solids

Takashi Kushida
Nara Institute of Science and Technology, Ikoma, Nara 630-0101, Japan

Masanori Tanaka*
Research Institute for Green Technology, National Institute of Advanced Industrial Science and Technology, Tsukuba, Ibaraki 305-8569, Japan

(Received 9 December 2001; published 2 May 2002)

The results of recent *ab initio* calculations performed by Smentek and Hess for several f-f transitions of Eu^{3+} in a host of C_{2v} symmetry are compared with experimental data, and dominant mechanisms of the $[^5D]_0$-$[^7F]_0$, $[^5D]_0$-$[^7F]_1$ and $[^5D]_1$-$[^7F]_0$ optical transitions of Eu^{3+} and Sm^{2+} ions are discussed. It is shown that the processes that were treated in the *ab initio* calculation make only very small contributions in these transitions in actual systems. The difference in the spectral shape of the $[^5D]_0$-$[^7F]_0$ line between Eu^{3+} and Sm^{2+} in glass is explained on the basis of the different dependence of the transition energy on the value of the crystal-field parameter B_{20}.

DOI: 10.1103/PhysRevB.65.195118 PACS number(s): 78.55.−m, 78.40.−q, 71.55.−i

I. INTRODUCTION

It is well known that most of the narrow spectral lines due to the optical transitions between the states of the $4f^N$ configuration of lanthanide ions in condensed matter are explained by the Judd-Ofelt theory.[1,2] In this theory, the electric-dipole transitions permitted by the odd-parity components of the crystal-field potential at the lanthanide ion site are treated by adopting the closure approximation. Then, it is found that the transition strength between the states $4f^N\Psi$ and $4f^N\Psi'$ is proportional to

$$\sum_{\lambda=2,4,6} \Omega_\lambda |\langle 4f^N\Psi' \| U^{(\lambda)} \| 4f^N\Psi\rangle|^2, \tag{1}$$

where $U^{(\lambda)}$ are unit tensor operators, while Ω_λ are so-called Judd-Ofelt parameters that depend on both host materials and lanthanide ions.

Since the spin-orbit interaction plays a significant role in lanthanide ions, let us use the intermediate coupling scheme and express a free-ion state as $[^{2S+1}L]_J$. It should be noted that S and L are not good quantum numbers. For example, the $[^5D]_J$ state of the Eu^{3+} ion contains considerable amount of the ^7F_J component in addition to the ^5D_J components.[3] When a lanthanide ion is placed in a host matrix, we must take into account the effects of the crystalline field acting on the lanthanide ion, although it is a good approximation to express a state by the free-ion wave function because these effects are small. The odd-parity terms of the crystal-field potential mix the higher $4f^{N-1}nd$ and $4f^{N-1}ng$ states into $4f^N$ states, thus partially allowing the electric-dipole transitions between two $4f^N$ states. As mentioned above, this process was theoretically treated by Judd[1] and Ofelt.[2]

Another important effect of the crystalline field is to mix two $4f^N$ states with different J values, which is called J mixing. In the Judd-Ofelt theory, this effect is not taken into account. Hence, J is a good quantum number, and we obtain the selection rule as

$$|J-J'| \leqslant \lambda \leqslant |J+J'|. \tag{2}$$

This means that the $J=0$-$J=0$, 0-1, 0-3, and 0-5 transitions are forbidden. In actual systems, however, spectral lines due to the transitions that violate the above condition (2) are sometimes observed. Typical examples are the $[^5D]_0$-$[^7F]_0$, $[^5D]_0$-$[^7F]_1$, $[^5D]_1$-$[^7F]_0$, $[^5D]_0$-$[^7F]_3$ and $[^5D]_3$-$[^7F]_0$ lines due to the transitions within the $4f^6$ configuration of Eu^{3+} and Sm^{2+} ions in several host materials. The mechanisms to allow these transitions have been discussed by several investigators.[4–12]

Recently, Smentek and Hess[13] reported an *ab initio* calculation of the $[^5D]_0$-$[^7F]_0$, $[^5D]_1$-$[^7F]_0$, $[^5D]_1$-$[^7F]_1$, $[^5D]_0$-$[^7F]_2$, $[^5D]_0$-$[^7F]_4$, and $[^5D]_2$-$[^7F]_0$ transition amplitudes of the Eu^{3+} ion in hosts with C_{2v} symmetry. The approach adopted is based on the second-order Judd-Ofelt theory modified by the third-order terms caused by the electron correlation effects among the $4f$ electrons of the lanthanide ion. They found that the matrix elements of two-particle effective operators, which represent electron correlation effects, determine the $[^5D]_0$-$[^7F]_0$ transition amplitude. For the $[^5D]_1$-$[^7F]_0$ and $[^5D]_1$-$[^7F]_1$ transitions, they employed the formulation that is based on the same physical model as the Judd-Ofelt theory but uses the velocity form of the electric-dipole interaction operator. From the numerical analyses, these authors obtained several results including the ratios of the transition amplitudes among the $[^5D]_0$-$[^7F]_0$, $[^5D]_1$-$[^7F]_0$ and $[^5D]_1$-$[^7F]_1$ transitions.

The purpose of this paper is to compare these results with experiments, and to discuss the dominant mechanisms of the 0-0 and 0-1 transitions of Eu^{3+} and Sm^{2+} ions in solids. We show that the contribution of the processes dealt with by Smentek and Hess[13] is negligibly small in actual systems. The asymmetric and nearly Gaussian spectral shapes of the $[^5D]_0$-$[^7F]_0$ lines of Eu^{3+} and Sm^{2+} in glass are discussed by taking into account the dependence of the transition energy on the axial second-rank crystal-field parameter B_{20} as well as the transition mechanism and the broad distribution of the value of B_{20}.

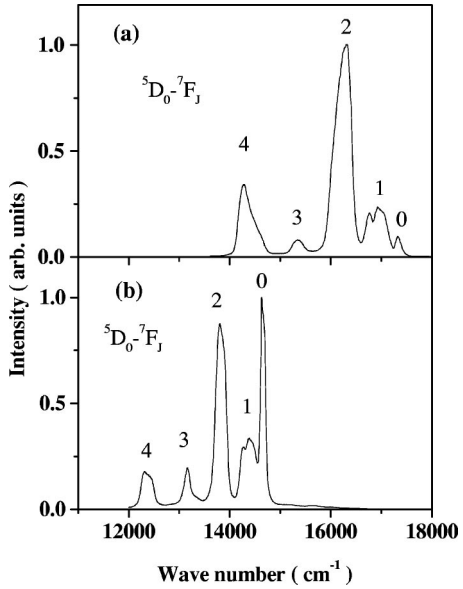

FIG. 1. Fluorescence spectra of (a) (80%) B_2O_3 and (20%) Na_2O glass containing 1 mole % of Eu^{3+} ions, and (b) (85%) B_2O_3, (10%) Na_2O, and (5%) Al_2O_3 glass containing 1 mole %, of Sm^{2+} ions at room temperature. The 322-nm light from a xenon lamp was passed through a monochromator (full width at half maximum: 6 nm) and used for the excitation.

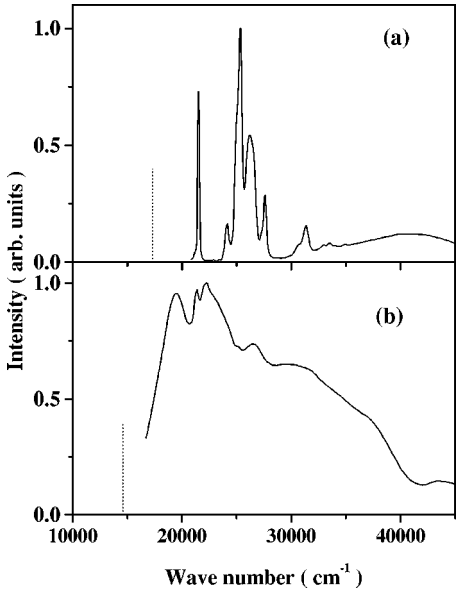

FIG. 2. Excitation spectra of (a) (80%) B_2O_3 and (20%) Na_2O glass containing 1 mole % of Eu^{3+} ions, and (b) (85%) B_2O_3, (10%) Na_2O, and (5%) Al_2O_3 glass containing 1 mole % of Sm^{2+} ions at room temperature. The intensities of the $[^5D]_0$-$[^7F]_2$ fluorescence of (a) Eu^{3+} and (b) Sm^{2+} ions were monitored. The dotted lines denote the positions of the $[^5D]_0$-$[^7F]_0$ line.

II. OPTICAL SPECTRA OF Eu^{3+} AND Sm^{2+} IONS IN OXIDE GLASS

As an example of the optical spectra of Eu^{3+} and Sm^{2+} ions in solids, we show the fluorescence and excitation spectra of these ions in oxide glass samples in Figs. 1 and 2. The $[^5D]_0$-$[^7F]_0$, $[^5D]_0$-$[^7F]_1$, and $[^5D]_0$-$[^7F]_3$ lines that are forbidden by the Judd-Ofelt theory are clearly observed in the fluorescence spectra. We notice that the intensity ratio between the $[^5D]_0$-$[^7F]_0$ and $[^5D]_0$-$[^7F]_1$ lines is much higher in Sm^{2+} compared with Eu^{3+}. The excitation spectra, which are considered to be almost the same as the absorption spectra, are quite different between the two samples. In Sm^{2+}-doped glass, the excitation band corresponding to the parity-allowed transition from the ground state to the $4f^5 5d$ states begins just above the $[^7F]_0$-$[^5D]_0$ line. In Eu^{3+}-doped glass, on the other hand, only the narrow lines due to the f-f transition of Eu^{3+} are observed up to $\sim 30\,000$ cm^{-1}. In this sample, the $4f^5 5d$ states lie above the charge-transfer states, and the excitation band corresponding to the transition to the charge-transfer state is observed around 40 000 cm^{-1}. In the following sections, we discuss the mechanisms of the 0-0 and 0-1 transitions and the spectral shape of the $[^7F]_0$-$[^5D]_0$ line of Eu^{3+} and Sm^{2+} ions.

III. THE 0-1 TRANSITION MECHANISM

First, let us consider the $[^5D]_0$-$[^7F]_1$ and $[^5D]_1$-$[^7F]_0$ transitions of the Eu^{3+} ion. It is well known that these 0-1 transitions are magnetic-dipole allowed. The magnetic-dipole transition between two states of the $4f^N$ configuration is parity allowed, and the J-selection rule is expressed, in a magnetic-dipole transition, as

$$\Delta J = 0, \pm 1 \quad (\text{except for } J=0\text{-}J=0). \tag{3}$$

Therefore, it is probable that the $[^5D]_0$-$[^7F]_1$ and $[^5D]_1$-$[^7F]_0$ transitions of Eu^{3+} are mainly due to magnetic-dipole transitions. When the Eu^{3+} ion is at a site having inversion symmetry, the $[^5D]_0$-$[^7F]_2$ transition is very weak in the fluorescence spectrum, while the intensity of the $[^5D]_0$-$[^7F]_1$ transition is comparable to that in the case of the Eu site of no inversion symmetry.[6] This indicates that the former transition is electric dipole in character, while the latter is magnetic dipole. Further, for the Eu^{3+} ions in $Ca(PO_3)_2$ glass, experiments on the polarization correlation between the excitation and fluorescence revealed that the $[^5D]_0$-$[^7F]_1$ and $[^5D]_1$-$[^7F]_0$ lines are due to magnetic-dipole transitions, while the $[^5D]_0$-$[^7F]_0$ and $[^5D]_1$-$[^7F]_1$ lines are due to electric-dipole transitions.[11,14] Polarization experiments to show similar results were also reported for the $EuAlO_3$ crystal.[8] Moreover, the strengths of the $[^7F]_0$-$[^5D]_1$ and $[^5D]_0$-$[^7F]_1$ transitions of Eu^{3+} in Y_2O_3 and $YAlO_3$ calculated under the assumption of the magnetic-dipole transition were reported to be in good agreement with experiments.[15,16] Thus, it is considered to be established that the $[^5D]_1$-$[^7F]_0$ and $[^5D]_0$-$[^7F]_1$ transitions of Eu^{3+} in various host materials are predominantly magnetic dipole. Therefore, we conclude that the electric-dipole transition dealt with by Smentek and Hess[13] in their *ab initio* calculation makes only a very small contribution in the $[^5D]_1$-$[^7F]_0$ and $[^5D]_0$-$[^7F]_1$ transitions of Eu^{3+}.

IV. THE 0-0 TRANSITION MECHANISM

A. Comparison of the results of *ab initio* calculation with experimental data

The $[^5D]_0$-$[^7F]_0$ line, which is strictly forbidden in free ions, is observed for Eu^{3+} and Sm^{2+} ions in several matrices. Smentek and Hess[13] treated it as the electric-dipole transition that becomes possible by the combination of the electron correlation effect and the linear crystal-field potential. From the results of numerical calculations for Eu^{3+} in a host with C_{2v} symmetry, they obtained the ratios of the transition amplitudes among the $[^5D]_0$-$[^7F]_0$, $[^5D]_1$-$[^7F]_0$ and $[^5D]_1$-$[^7F]_1$ transitions as follows:

$$T([^5D]_1\text{-}[^7F]_0)/T([^5D]_0\text{-}[^7F]_0)=43,$$

$$T([^5D]_1\text{-}[^7F]_1)/T([^5D]_0\text{-}[^7F]_0)=25,$$

$$T([^5D]_1\text{-}[^7F]_1)/T([^5D]_1\text{-}[^7F]_0)=0.58.$$

These ratios are independent of the values of the crystal-field parameters so long as B_{10} is nonzero, because all the three transition amplitudes are proportional to the crystal-field parameter B_{10}. For the $[^5D]_1$-$[^7F]_0$ and $[^5D]_1$-$[^7F]_1$ transitions, they employed the alternative formulation of the second-order theory based on the velocity form of the electric-dipole interaction operator.

We can estimate the significance of the electric-dipole transitions treated in these *ab initio* calculations from the above ratios. In the preceding section, we showed that the $[^5D]_1$-$[^7F]_0$ transition observed in actual systems are predominantly magnetic dipole in character, and the contribution of the electric-dipole process dealt with by Smentek and Hess[13] is very small in this transition. From the above ratio, the amplitude of the $[^5D]_1$-$[^7F]_1$ transition is comparable to that of the electric-dipole $[^5D]_1$-$[^7F]_0$ transition. Therefore, we conclude that the $[^5D]_1$-$[^7F]_1$ transition that was considered in the *ab initio* calculation is very weak compared with the magnetic-dipole $[^5D]_1$-$[^7F]_0$ transition. The strength of the $[^5D]_1$-$[^7F]_1$ transition of Eu^{3+} in the site of no inversion symmetry is usually comparable to that of the $[^5D]_1$-$[^7F]_0$ transition. Thus, the $[^5D]_1$-$[^7F]_1$ transition treated by Smentek and Hess is concluded to be insignificant in actual systems. Further, we can say that the $[^5D]_0$-$[^7F]_0$ transition caused by the third-order terms due to the electron correlation effect is negligible, because, from the above ratio, the transition strength of this process is about 1/2000 of that of the electric-dipole $[^5D]_1$-$[^7F]_0$ transition.

B. Probable mechanisms of the 0-0 line

Three probable mechanisms have been proposed for the $[^5D]_0$-$[^7F]_0$ transition of Eu^{3+} and Sm^{2+} in the literature; namely, (i) the breakdown of the closure approximation adopted in the Judd-Ofelt theory,[4,5,9] (ii) Wybourne-Downer mechanism that involves spin-orbit linkages within excited configurations,[7,17,18] and (iii) borrowing of intensity from other transitions by J mixing.[7,8,10–12] These processes were not taken into account in the *ab initio* calculation by Smentek and Hess.[13] The $[^5D]_0$-$[^7F]_0$ line due to the mechanism (i) appears only when the crystal-field expansion contains a linear term, and the breakdown of the closure approximation is significant when the energy of the higher opposite-parity states to mix into $4f^N$ states is low. In the Eu^{3+} ion, the charge-transfer state is known to lie at relatively low energies.[19] Hence, it is possible that the admixture of this state plays an essential role in the electric-dipole f-f transitions of Eu^{3+}.[9] However, as mentioned below, the contribution of the breakdown of the closure approximation is generally considered to be small.

In the excited-state spin-orbit interaction mechanism (ii), the 0-0 transition is allowed even if the closure approximation is adopted.[7,17] A linear term of the crystal-field potential is again necessary for the $[^5D]_0$-$[^7F]_0$ transition by this mechanism. It is known that the $[^5D]_0$-$[^7F]_0$ transition strength is much larger in Sm^{2+} compared with the isoelectronic Eu^{3+} in various host matrices.[20–22] This is true also in the case of glass hosts as seen in Fig. 1. It should be noted that the intensity of the $[^5D]_0$-$[^7F]_1$ fluorescence can be used as a standard, because this is due to the allowed magnetic-dipole transition and accordingly its strength is insensitive to the host material. Further, this strength is almost the same for Eu^{3+} and Sm^{2+}, because the wave functions of the states concerned are almost the same in these ions. The $4f^55d$ states of Sm^{2+} are located much lower in energy than the charge-transfer states of Eu^{3+} (cf. Fig. 2), and the energy difference between the higher opposite-parity states and the $4f^N$ states appears twice in the denominator of the transition matrix element of the mechanism (ii), while only once in the case of (i). Therefore, the above-mentioned fact is interpreted in terms that the mechanism (ii) is dominant in the $[^5D]_0$-$[^7F]_0$ transition of Sm^{2+}.[21,22]

The 0-3 and 0-5 transitions are forbidden by the Judd-Ofelt theory. Further, these transitions due to the Wybourne-Downer mechanism are known to be very weak.[18] Since the $[^5D]_0$-$[^7F]_3$ transition is not much enhanced in Sm^{2+} compared with Eu^{3+} in glass (cf. Fig. 1), we consider that the contribution of the breakdown of the closure approximation in the Judd-Ofelt theory is not significant in these ions. Therefore, we infer that the mechanism (ii) and/or (iii) make the dominant contribution in the 0-0 transition of Eu^{3+} and Sm^{2+} in various host materials. It should be noted that the linear term is not necessary in the crystal-field expansion in the mechanism (iii).

The $[^5D]_0$-$[^7F]_2$ and $[^5D]_0$-$[^7F]_4$ transitions are allowed by both Judd-Ofelt and Wybourne-Downer mechanisms. In these transitions, however, the enhancement due to the presence of the $4f^55d$ states in the vicinity of the $4f^6$ states concerned with the transitions is not observed for the Sm^{2+} ions in solids. This was identified as due to the destructive interference between the contributions of the above two mechanisms.[22] In contradiction to the criticism of Smentek and Hess,[13] no unknown parameters were obtained from a fitting procedure in deriving this conclusion. Smentek[23] mentioned that our calculation[22] taking into account only the $4f^55d$ states of Sm^{2+} as the excited states to mix into the $4f^6$ configuration states is not accurate and the contributions of other excited states that are allowed by parity are not negligible. However, the fact that the $4f^55d$ states of Sm^{2+}

are extremely low in energy compared with other excited configuration states was not taken into account.

C. The 0-0 transition due to *J* mixing in Eu^{3+}-doped glass

From the weak intensity of the $[^5D]_0$-$[^7F]_3$ transition of Eu^{3+} ions in various host materials, the *J*-mixing effect has been believed to be generally small. In the case of glass doped with Eu^{3+}, however, we found that this effect plays a dominant role in the $[^5D]_0$-$[^7F]_0$ transition.[10–12] Glass doped with Eu^{3+} ions usually shows red fluorescence due to the transitions from the $[^5D]_0$ state to the lower $[^7F]_J$ states. Detailed studies of this fluorescence were carried out on Eu^{3+}-doped $Ca(PO_3)_2$ glass using a site-selective spectroscopic technique.[10,11,24] It has been found from the polarization experiment that the Eu site has C_{2v} or C_2 point symmetry in this glass.[11] The broad line around 590 nm, which is asymmetric in shape with a longer tail in the high-energy side, is assigned to the $[^5D]_0$-$[^7F]_0$ transition. The spectral shape of this line is almost the same between the absorption and fluorescence under broadband light excitation, and fluorescence line narrowing is observed when the sample is excited with monochromatic light in the energy region of this line. This means that this line is inhomogeneously broadened because of the distribution of the crystal-field strength in glass.

From the energy splitting of the $[^7F]_1$ manifold determined from the laser-induced fluorescence spectra under various excitation wavelengths, it was found that the value of the crystal-field parameter B_{20} has a broad distribution and the spread of the energy difference between the $[^5D]_0$ and $[^7F]_0$ states is determined by the spread of this value.[10–12] We further found that the $[^5D]_0$-$[^7F]_0$ transition strength is linearly dependent on the transition energy under site-selective excitation.[10–12] This result is interpreted in terms that the $[^7F]_0$ state is pushed downwards by the mixing of the $M_J=0$ level of the $[^7F]_2$ manifold into $[^7F]_0$ through the axial second-rank crystal-field component $B_{20}C_0^{(2)}=(4\pi/5)^{1/2}B_{20}Y_{20}$ (Y_{20} is the spherical harmonics), while the $[^5D]_0$-$[^7F]_0$ transition is partially allowed by the borrowing of intensity from the $[^5D]_0$-$[^7F]_2$ ($M_J=0$) line through the same mixing.[10–12] Because both the energy shift and the transition strength of the $[^5D]_0$-$[^7F]_0$ line are linearly dependent on B_{20}^2, the linear correlation between the transition strength and the energy position of this line can be explained.

This $[^5D]_0$-$[^7F]_0$ transition mechanism of Eu^{3+} in $Ca(PO_3)_2$ glass has been confirmed by the observation that the degree of linear polarization of fluorescence is as high as 0.5, as expected for the above mechanism, for the 0-0 resonance fluorescence under linearly polarized light excitation,[14] and also by the fact that the intensity ratio of the $[^5D]_0$-$[^7F]_0$ to the $[^5D]_0$-$[^7F]_2$ transition is in good agreement with the ratio calculated using the value of B_{20} obtained from the splitting of the $[^7F]_1$ manifold.[11,12] It has also been shown that the mixing of the $[^7F]_2$ into $[^7F]_0$ through the second-rank crystal-field potential $V_c^{(2)}=\Sigma_q B_{2q}C_q^{(2)}$ plays a dominant role in the vibronic spectra of the $[^5D]_0$-$[^7F]_0$ and $[^5D]_1$-$[^7F]_0$ transitions of Eu^{3+} in oxide glasses.[25] We also found that the *J* mixing affects the mean energy of the $[^7F]_1$ manifold[11,12,21] and also the homogeneous width of the $[^5D]_0$-$[^7F]_0$ line[26] in Eu^{3+} and Sm^{2+} ions in glass. On the other hand, Schmidt *et al.*[27] showed that the nuclear quadrupole splitting of the $[^7F]_0$ state of Eu^{3+} in silicate glass increases linearly with the excitation energy in the $[^7F]_0$-$[^5D]_0$ absorption band. This can also be explained by the crystal-field-induced mixing of $[^7F]_2$ into $[^7F]_0$.[28]

Wybourne[7] mentioned that the excited-state spin-orbit coupling mechanism (ii) would be dominant for the 0-0 transition of Sm^{2+}, while the *J*-mixing mechanism due to the admixture of $[^7F]_2$ into $[^7F]_0$ would be dominant in the case of Eu^{3+}. Our experimental results on glass samples are in good agreement with these interpretations. However, this *J*-mixing mechanism is not always dominant for the 0-0 transition of Eu^{3+} in various hosts. For example, we found that this mechanism is not important in the case of Eu^{3+} in polyvinyl alcohol and Y_2O_2S crystal powder from the $[^5D]_0$-$[^7F]_0$ to $[^5D]_0$-$[^7F]_2$ fluorescence intensity ratio and the dependence of the 0-0 transition strength on the value of B_{20}.[12] In these samples, the Wybourne-Downer mechanism is probably dominant.

In the *ab initio* calculation, Smentek and Hess[13] found that the expression for the $[^5D]_0$-$[^7F]_0$ transition amplitude has the form that can be interpreted in terms of the borrowing of intensity from other states through the Coulomb interaction operator. A numerical calculation showed that many excited states with $J=2$, 4, and 6 contribute to the borrowing. Therefore, these authors concluded that the scheme of borrowing intensity is rather complex and it is impossible to distinguish a single term that is dominant. However, their conclusion was obtained for the electric-dipole 0-0 transition through the electron correlation effect, and as mentioned above, various results clearly show that the mixing of the $[^7F]_2$ ($M_J=0$) state into $[^7F]_0$ contributes dominantly to the $[^5D]_0$-$[^7F]_0$ transition in the case of Eu^{3+}-doped $Ca(PO_3)_2$ glass.

Smentek and Hess[13] mention that they do not compare their results with the analysis of Kushida and his co-workers, because their *ab initio* results have been obtained for the complete radial basis sets of one-electron functions, while the excitations are limited at most to the first excited states of *d* and *g* symmetries in the latter analysis. This is not correct. In our model, the $[^5D]_0$-$[^7F]_0$ transition borrows intensity from the $[^5D]_0$-$[^7F]_2$ transition. In this case, the excited states that mix by the odd-parity crystal-field potential and enable the electric-dipole $[^5D]_0$-$[^7F]_2$ transition are not limited to the $4f^55d$ and $4f^55g$ states, but higher states are also included. Further, even the contribution of the charge-transfer states, which was not taken into account by Smentek and Hess, and also the contributions to explain the hypersensitive enhancement of the $[^5D]_0$-$[^7F]_2$ line, such as due to the ligand polarization[29] are not excluded.

V. SPECTRAL SHAPE OF THE 0-0 LINE OF Eu^{3+} AND Sm^{2+} IN GLASS

The solid lines in Figs. 3 and 4 show the $[^5D]_0$-$[^7F]_0$ fluorescence spectra under the broadband light excitation of

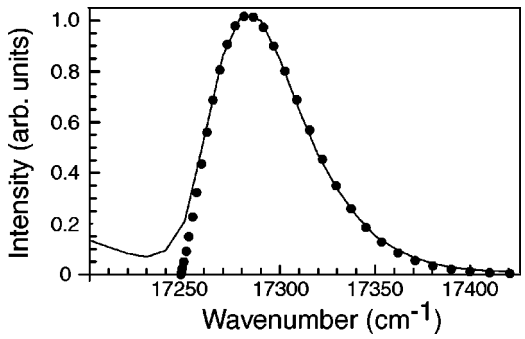

FIG. 3. The $[^5D]_0$-$[^7F]_0$ fluorescence spectrum of Eu^{3+} in $Ca(PO_3)_2$ glass at 77 K excited by ultraviolet light from a deutrium lamp (Ref. 24). The closed circles show the theoretical curve calculated using Eqs. (5), (6) and (7) with $X_m=-620$ cm^{-1} and $\sigma=271$ cm^{-1}.

Eu^{3+} and Sm^{2+} ions in glass. We notice that the line shape is asymmetric in Eu^{3+}, while it is almost symmetric in Sm^{2+}. The asymmetric spectral shape of the $[^5D]_0$-$[^7F]_0$ line is often observed in Eu^{3+}-doped glass. In both cases of Figs. 3 and 4, the $[^5D]_0$-$[^7F]_0$ line is inhomogeneously broadened and it is attributable to the distribution of the values of the second-rank crystal-field parameters. The values of B_{20} and $|B_{22}|$ at various sites can be determined from the energy separations among the three $[^5D]_0$-$[^7F]_1$ fluorescence lines under site-selective excitation. It is known that the value of $|B_{22}|$ is almost insensitive to the 0-0 transition energy in these samples.[11,22]

Figure 5 shows the relation between the value of B_{20} and the transition energy of the 0-0 line for Eu^{3+} in $Ca(PO_3)_2$ glass. As shown by a dashed line in Fig. 5, the 0-0 transition energy E is expressed, as a function of $X\equiv B_{20}$, as

$$E=aX^2+c. \tag{4}$$

If we assume that the energy of the $[^7F]_0$ state is affected only by the mixing of $[^7F]_2$ due to the second-rank crystal-field potential $V_c^{(2)}$, while the energy of the $[^5D]_0$ state is independent of $V_c^{(2)}$, a is calculated to be $4/75\Delta_{20}$.[11] With

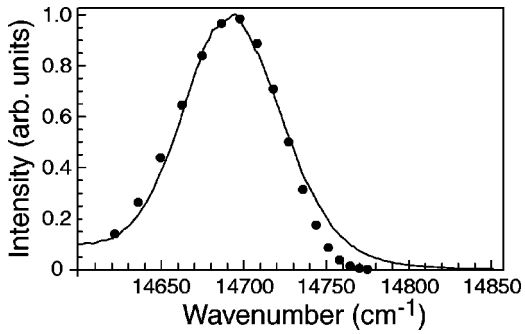

FIG. 4. The $[^5D]_0$-$[^7F]_0$ fluorescence spectrum of Sm^{2+} in (28.2) AlF_3- and (12.2) HfF_4-based glass that contains (8.3) YF_3, (3.5) MgF_2, (18.3) CaF_2, (13.1) SrF_2, (12.6) BaF_2, and (3.8) NaF as all concentrations expressed as modifiers (mole %) at 77 K. All lines of an Ar^+ ion laser were used for the excitation. The closed circles show the theoretical curve calculated using Eqs. (5), (6) and (7) with $X_m=-560$ cm^{-1} and $\sigma=141$ cm^{-1}.

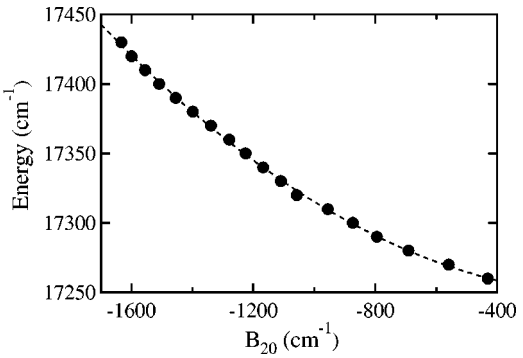

FIG. 5. The transition energy of the $[^5D]_0$-$[^7F]_0$ line versus B_{20} for Eu^{3+} in $Ca(PO_3)_2$ glass at 77 K. The closed circles show the data obtained from Fig. 1 of Ref. 24. The dashed line denotes the curve calculated through Eq. (4) with $a=6.75\times10^{-5}$ cm and $c=17\,248$ cm^{-1}.

the energy difference $\Delta_{20}=920$ cm^{-1} between the $[^7F]_2$ and $[^7F]_0$ states,[11] this gives $a=5.8\times10^{-5}$ cm, which is in fair agreement with the value obtained in Fig. 5. The small difference might be due to the mixing of other states such as even-parity charge-transfer states into $[^7F]_0$ through $V_c^{(2)}$.[9,24]

In the case of Sm^{2+}-doped fluoride glass, on the other hand, it is not possible to express the energy E by Eq. (4), and as seen in Fig. 6, it is necessary to use such an expression as

$$E=a(X+b)^2+c. \tag{5}$$

The value of a is negative and b is large, which disagree with the expectation under the assumption that the energy of the $[^5D]_0$ state is independent of $V_c^{(2)}$. This might be due to the presence of the $4f^55d$ states in the vicinity of $[^5D]_0$.

We calculated the $[^5D]_0$-$[^7F]_0$ fluorescence spectra using the following relation:

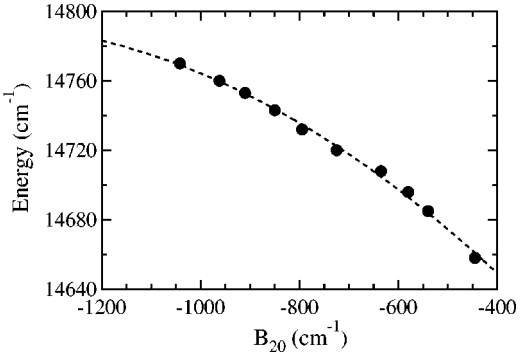

FIG. 6. The transition energy of the $[^5D]_0$-$[^7F]_0$ line versus B_{20} for Sm^{2+} in (28.2) AlF_3- and (12.2) HfF_4-based glass that contains (8.3) YF_3, (3.5) MgF_2, (18.3) CaF_2, (13.1) SrF_2, (12.6) BaF_2, and (3.8) NaF at 77 K. The closed circles show the data obtained from Fig. 5 of Ref. 21. The dashed line denotes the curve calculated through Eq. (5) with $a=-1.22\times10^{-4}$ cm, $b=1485$ cm^{-1}, and $c=14\,793$ cm^{-1}.

$$F(E)=\int EP(X)Z\delta[E-a(X+b)^2-c]dX, \qquad (6)$$

where the distribution of the value of X in glass was assumed to be a Gaussian as

$$P(X)=(2\pi\sigma^2)^{-1/2}\exp[-(X-X_m)^2/2\sigma^2], \qquad (7)$$

and lanthanide ions in various sites were assumed to be uniformly excited. The homogeneous broadening of the $[^5D]_0$-$[^7F]_0$ line was neglected because it is small. Further, the site-to-site variation of $|B_{22}|$ was not taken into account for simplicity. We put $Z=X^2$ and $b=0$ for Eu^{3+}-doped glass assuming the above-mentioned intensity-borrowing mechanism. On the other hand, we put $Z=1$ for Sm^{2+}-doped glass, because the Wybourne-Downer mechanism is considered to be dominant. The closed circles in Figs. 3 and 4 show the spectra thus calculated. The agreement between the calculation and experiment is satisfactory in the case of Eu^{3+} in glass, while it is fair for Sm^{2+}. The origin of the discrepancy in the latter is not clear. The fitting curve for Sm^{2+} in glass obtained using $Z=X^2$ was almost the same as that in Fig. 4. The discrepancy between the calculation and experiment in Fig. 4 may be explained by the divergence of the distribution of the value of B_{20} from a Gaussian, the nonuniform excitation of the lanthanide ions, and the temporal variation of the crystal-field strength in glass[30] due to the large time difference between the measurements of the 0-0 lineshape and the data of Fig. 5 of Ref. 21. Anyway, from the results in Figs. 3 and 4, we see that the asymmetric 0-0 line shape of Eu^{3+} and nearly symmetric shape of Sm^{2+} are explained well by taking into account the dependence of the transition energy E on the value of B_{20} and the broad distribution of this value. It has already been reported that this type of calculation reproduces the 0-0 fluorescence line shape of Eu^{3+} in glass.[31] In Ref. 24, on the other hand, the distribution of the value of $|B_{22}|$ was also taken into account in the fitting of the 0-0 line shape of Eu^{3+} in glass. However, since the mean value of $|B_{22}|$ is almost insensitive to the 0-0 transition energy, the essential point of the asymmetric spectral shape is reproduced well by Eqs. (6) and (7) as seen in Fig. 3.[32]

VI. SUMMARY

The electric-dipole $[^5D]_0$-$[^7F]_0$, $[^5D]_0$-$[^7F]_1$, and $[^5D]_1$-$[^7F]_1$ transitions of Eu^{3+} ions treated in the *ab initio* calculation of Smentek and Hess[13] have been shown to be insignificant in actual systems. The dominant mechanisms of the 0-0 and 0-1 transitions in Eu^{3+} and Sm^{2+} have been discussed, and the significance of the intensity borrowing mechanism through J mixing for the $[^5D]_0$-$[^7F]_0$ transition of Eu^{3+} in glass has been emphasized. The different spectral shapes of the 0-0 line in Eu^{3+} and Sm^{2+} have been explained by taking into account the difference in the relation between the transition energy and the value of B_{20}.

*Fellow, New Energy and Industrial Technology Development Organization.

[1] B. R. Judd, Phys. Rev. **127**, 750 (1962).
[2] G. S. Ofelt, J. Chem. Phys. **37**, 511 (1962).
[3] G. S. Ofelt, J. Chem. Phys. **38**, 2171 (1963).
[4] Z. J. Kiss and H. A. Weakliem, Phys. Rev. Lett. **15**, 457 (1965).
[5] W. C. Nieuwpoort and G. Blasse, Solid State Commun. **4**, 227 (1966).
[6] G. Blasse, A. Bril, and W. C. Nieuwpoort, J. Phys. Chem. Solids **27**, 1587 (1966).
[7] B. G. Wybourne, in *Optical Properties of Ions in Crystals*, edited by H. M. Crosswhite and H. W. Moos (Interscience, New York, 1967), p. 35.
[8] M. Kajiura and K. Shinagawa, J. Phys. Soc. Jpn. **28**, 1041 (1970).
[9] T. Hoshina, S. Imanaga, and S. Yokono, J. Lumin. **15**, 455 (1977).
[10] G. Nishimura and T. Kushida, Phys. Rev. B **37**, 9075 (1988).
[11] G. Nishimura and T. Kushida, J. Phys. Soc. Jpn. **60**, 683 (1991).
[12] M. Tanaka, G. Nishimura, and T. Kushida, Phys. Rev. B **49**, 16 917 (1994).
[13] L. Smentek and B. A. Hess, Jr., Mol. Phys. **92**, 835 (1997).
[14] T. Kushida, E. Takushi, and Y. Oka, J. Lumin. **12/13**, 723 (1976).
[15] W. F. Krupke, Phys. Rev. **145**, 325 (1966).
[16] M. J. Weber, T. E. Varitimos, and B. H. Matsinger, Phys. Rev. B **8**, 47 (1973).
[17] M. C. Downer, G. W. Burdick, and D. K. Sardak, J. Chem. Phys. **89**, 1787 (1988).
[18] G. W. Burdick, M. C. Downer, and D. K. Sardak, J. Chem. Phys. **91**, 1511 (1989).
[19] C. K. Jørgensen, R. Pappalardo, and E. Rittershans, Z. Naturforsch. **20A**, 54 (1964).
[20] L. L. Chase, S. A. Payne, and G. D. Wilke, J. Phys. C **20**, 953 (1987).
[21] M. Tanaka and T. Kushida, Phys. Rev. B **49**, 5192 (1994).
[22] M. Tanaka and T. Kushida, Phys. Rev. B **53**, 588 (1996).
[23] L. Smentek, Phys. Rep. **297**, 155 (1998).
[24] G. Nishimura and T. Kushida, J. Phys. Soc. Jpn. **60**, 695 (1991).
[25] M. Tanaka and T. Kushida, Phys. Rev. B **60**, 14 732 (1999).
[26] M. Tanaka and T. Kushida, Phys. Rev. B **52**, 4171 (1995).
[27] Th. Schmidt, R. M. Macfarlane, and S. Völker, Phys. Rev. B **50**, 15 707 (1994).
[28] R. J. Elliot, Proc. Phys. Soc. London, Sect. B **70**, 119 (1957).
[29] S. F. Manson, R. D. Peacock, and B. Stewart, Mol. Phys. **30**, 1829 (1975).
[30] E. Takushi, K. Hirata, and T. Sasaya, Proc. Jpn. Acad., Ser. B: Phys. Biol. Sci. **61**, 49 (1985).
[31] T. Kushida and G. Nishimura, J. Lumin. **40/41**, 111 (1988).
[32] In Refs. 24 and 31, $F(E)$ was assumed to be proportional to the spontaneous emission rate that contains a factor E^3. However, since the fluorescence efficiency is very high in Eu^{3+}- and Sm^{2+}-doped glasses, we have omitted this factor in Eq. (6).